Automatic preform design and optimization for aeroengine disk forgings

yan han
Menghan Wang (cquwmh@163.com)
College of Materials Science and Engineering of Chongqing University
yifeng chen
mingfei chen
xiang xiang

Research Article

Keywords: Preform optimal design, Cooperative simulation, NURBS curve, Genetic algorithm

Posted Date: May 18th, 2022

DOI: https://doi.org/10.21203/rs.3.rs-1653145/v1

Automatic preform design and optimization for aeroengine disk forgings

Yan Han[1] · Menghan Wang[*1]· Yifeng Chen[1] ·Mingfei Chen[1] · Xiang Xiang[1]

Abstract

To ensure a more uniform microstructure distribution of forging and improve the service performance of aeroengine disk parts, an automated preform design method is proposed for integrated preform shape design and optimization based on the NURBS curve, finite element method (FEM), and genetic algorithm (GA). Firstly, the random preform shape graph is automatically constructed by the NURBS curve design criterion. The volume and shape complexity are used as the constraints of the preform. Then the ratio of the mesh area within the set strain range to the total mesh area is used as the fitness function for the uniformity of deformation, and the genetic algorithm module is used for optimization. Finally, a large disk forging is an example of its optimal design. The results show that the deformation uniformity of the forgings is excellent, its fitness value is as high as 99.59%, and there are no problems such as folding, underfilling, and limited distribution of flash, which verifies the effectiveness of the method. In addition, the method has the advantage of strong universality, which can find the preform shape with good deformation uniformity for any shape forgings.

Keywords Preform optimal design · Cooperative simulation · NURBS curve · Genetic algorithm

1 Introduction

In Aeroengines, many disk forgings are formed by the forging process [1,2]. Their performance and life determine the performance and life of the engine and indirectly affect the performance of the whole engine [3]. Since disk forgings need to work under severe service conditions, higher requirements are placed on their forgings' organizational and mechanical properties [1, 4]. Uniform distribution of deformation is one of the essential requirements for aerospace forgings [5]. While reducing the forming load [6-8] and eliminating the forming defects such as underfilling [9-11], folds [9,11,12], and cracks [13-15], the deformation uniformity should also be guaranteed. The uniformity of deformation inside the forging directly determines the uniformity of forging organization [8, 16], and forging internal organization is uniformly distributed by the deformation uniformity decision, and non-uniform organization will lead to reduced fatigue life of forgings or premature failure in the process of use. Mixed crystal and coarse grains are the primary organizational defects [17-19]. To ensure high-quality forging, the design and optimization of the preform for disk forgings are critical.

Some methods are used to design preform shapes. The upper bound element technique (UBET) is commonly used in the backward simulation. It is widely used for designing preforms for axisymmetric parts due to its simple principle and fast solution speed [20-22]. Another method used in the backward simulation is based on the boundary node release criterion and backtracking loading path to determine the appropriate precast design, i.e., Backward tracing scheme (BTS) [23,24], and this method has been successfully applied to design the preform die-shapes of a generic turbine-disk forging process [24]. The equipotential field method is also a preform design technique used in the material forming [25-27]. Its design is based on the similarity principle, which determines the preform shape of the forging based on the equipotential line between the initial shape and the final shape [28]. In addition, it is possible to use other physical fields to describe the material flow and thus obtain the shape of the preform, for example, by integrating QForm metal forming simulation software with special CAD software that enables isothermal surface extraction to preform modeling [27]. With the development of random computer technology, a preform shape design method based on optimal design is widely used, which is to optimize the design variables related to the preform shape size to get the optimal solution with a particular index or a specific relative relationship as the objective function, such as response surface method (RSM) [29-31], sensitivity analysis [32,33], genetic algorithms (GA) [34-36], topological optimization [37,38] and reduced basis technique (RBT) [39].

[*] Menghan Wang cquwmh@163.com

[1] School of Materials Science and Engineering, Chongqing University, Chongqing 400030, China

The preform shape, no matter what design method is used to obtain it, needs to be verified by the forward forming process [27,31,36,38]. The difficulty of forwarding process analysis is parameter setting and constraint control, which reduces the number of trials and errors and improves optimization efficiency. However, it is undeniable that both UBET, BTS, sensitivity analysis, and topological optimization require user technicians to consider the forgings' structural features and metal flow characteristics, which is a tedious process and consumes a lot of time and effort. And, the above methods require preliminary guesses on the preform design during the design variables. The optimization results inevitably have certain user biases and cannot search for potential preform shapes [7]. Based on the above problems, there is a growing need for an engineering method that can be used by simply telling the system basic information about the forgings. The system will automatically complete the design and optimization of the preforms.

After considering the limitations of current preform design methods, an integrated system is developed to obtain satisfactory preforms in this paper. Firstly, the appropriate strain range is selected according to the forging requirements. A suitable fitness function is established. The corresponding solution algorithm is built based on the direct communication between finite element analysis and the genetic algorithm. Secondly, the NURBS curves are used to describe the shape of the preform, the positions of the control points are defined as design variables, and the GA is used as a controller to control these design variables to obtain a satisfactory preform shape by crossover, variation, and competition among all individuals. Finally, the feasibility of the optimization algorithm is verified with two disk forges. In addition, the optimal preform shapes obtained by the algorithm are redesigned to derive shapes that can be used in actual production.

2 Design of algorithm for preform optimization

2.1 Design of objective function

According to the general forming process, the forgings are formed by preform, and then the forgings are machined to obtain the finished part, as shown in the white box in Fig. 1. In this study, the equivalent effect field indicates the deformation uniformity. In the actual production, to ensure the mechanical properties and microstructure of the aeroengine rotary forgings meet the requirements, it is required that the equivalent effect variation value of finished parts is 0.43~1.02.

To accurately judge the forming effect of forgings by computer, it is necessary to quantify the equivalent strain field of the finished parts. The essence of an equivalent strain field is the combination of equivalent strain values for each grid element [31]. By extracting and calculating, the ratio of the grid area within the set strain range to the total grid area can accurately judge whether the forming effect is good or not. The larger the ratio, the better the forming product, and vice versa, the worse it is, calculated as in equation (1):

$$F_s = -\frac{\sum_{i=1}^{n} S_i}{\sum_{i=1}^{m} S_i} \tag{1}$$

Where F_s is the objective function to achieve the ratio of the grid area to the total grid area in the set strain range. n is the number of grids that reach the set strain range. m is the total grid number. and S_i is the corresponding grid area under a certain grid number. The range of fitness value F_s is from zero to one.

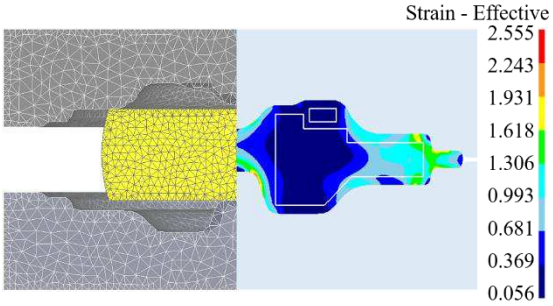

Fig. 1 Schematic diagram of forging structure

Die filling is considered one of the optimization objectives, although it must be quantified to apply in the data analysis process [40]. A filling ratio parameter was introduced to quantify die-filling, as follows:

$$FR = \frac{V_{actual}}{V_{\text{forge}}} \tag{2}$$

Where V_{forge} and V_{actual} is the volume of the final forging part before and after trimming flash respectively. There is no underfilling situation, and the filling rate can be idealized to 1. Here $V_{actual} = V_{\text{forge}}$.

Flash volume is obtained by Eq. 2:

$$FV = V_{pre} - V_{forge} \tag{3}$$

Where V_{pre} is the volume of the preform. Here, the flash volume is only used as a constraint on the fitness function F_s.

2.2 Random Preform design based on NURBS curve

Design principle

After obtaining the evaluation index, it is necessary to construct a series of preform shapes to find the optimal individual by the optimistic algorithm. It is well known that NURBS (Non-Uniform Rational B-Spline) is a handy tool for geometric modeling and is gained more and more attention from the engineering community for its good properties [41]. Since NURBS has the characteristics of manipulating control points and weighting factors, which can provide sufficient flexibility for the shape design of preforms with various complex shapes. NURBS modeling is always defined by curves and surfaces so that sharp corners will not be generated, which the preform expects. On the one hand, sharp corners will cause the folding of forgings. On the other hand, it will increase the number of

remeshing in finite element simulation and reduce computational efficiency. The NURBS curve describes the outline of the preform (see Fig. 2).

The expression of the NURBS curve equation is

$$p(u) = \frac{\sum_{i=0}^{n} \omega_i p_i N_{i,k}(u)}{\sum_{i=0}^{n} \omega_i N_{i,k}(u)}, u \in [0,1] \quad (4)$$

Here, $N_{i,k}(u)$ mainly refers to the basic function of k times B-sample. p_i denotes the control point. ω_i denotes the weight factor of the control vertex p_i, and the size of ω_i value determines the degree of curve deviation from the control point, see Fig. 2(a), where ω_1 is smaller than ω_2, ω_2 is smaller than ω_3, and the larger of ω_i represents the more significant weight factor, the closer the curve is to the control point p_i, that the shape of the NURBS can be changed to approximate any shape by adjusting its control points, which is extremely important for various aspects of subsequent graph redesign, analysis, and processing.

From Fig. 2(a), it can be observed that the x-coordinate of the data point is relatively fixed, and its length is limited by the maximum radius length of the forging. Here, its y-coordinate is defined as a design variable so that the shape of the preform can be changed in a wide range, thus screening out some potential preform shapes, see Fig. 2(b). Therefore, the shape optimization problem can be transformed into a parameter optimization problem.

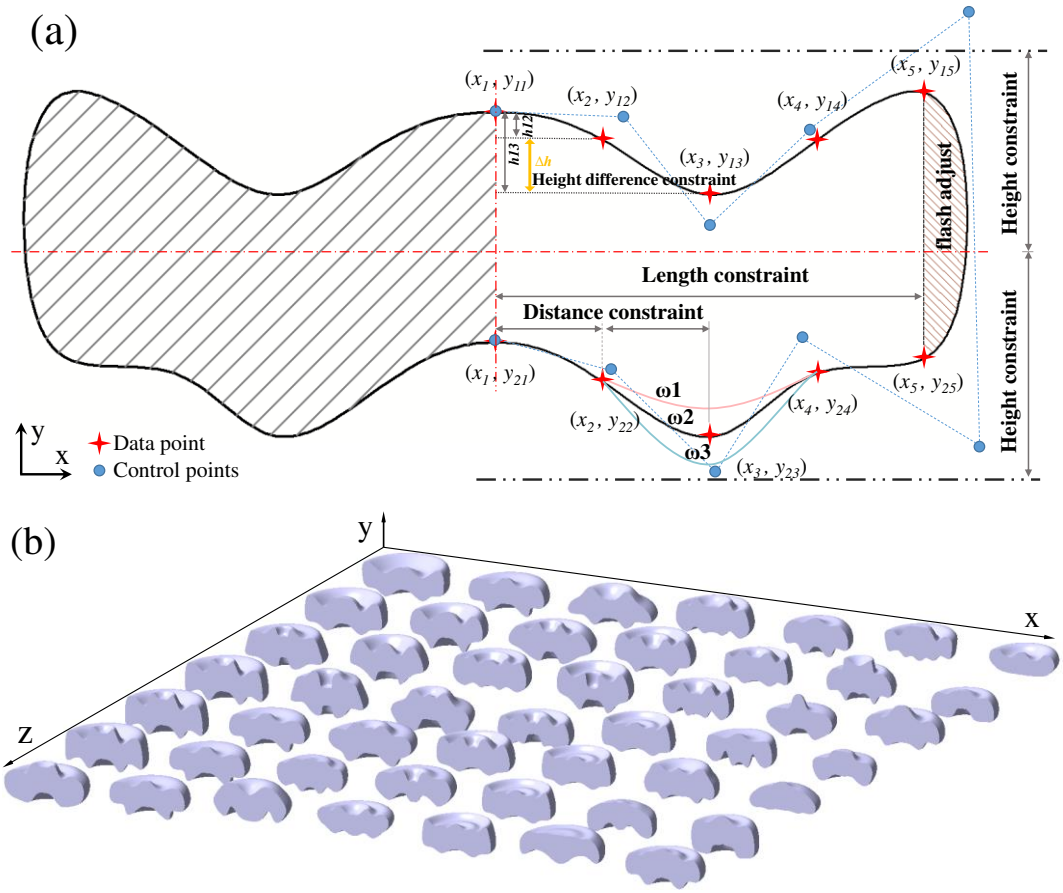

Fig. 2 Random preform modeling diagram: (a) NURBS curve constraint diagram; (b) Random preform modeling diagram

Shape constraint

As shown in Fig. 2, the random preform graph generated by the NURBS curve consists of two curves on the top and bottom and a raised arc on the right side, where the two unexpected curves are divided by the x-axis and are generated by interpolating two or more reference points, respectively. Since the values of the reference points are strongly random, they also need to be subject to certain constraints.

In the actual forging process, the length of the preform shape is shorter than the length of the forging. The design length of the preform is highly related to the maximum length of the forging. This work sets the maximum length of the curve in the x-axis direction to 'm times the maximum radius length of the forging (5) '. The distance between each reference point is assigned according to the number of reference points (6). The distance between each reference point can be customized.

$$x_{pre} = m * l_{max} \quad m \in [0.6, 0.8] \quad (5)$$

$$x_{distance} = l_{max} / n \quad (6)$$

Where x in Eq. (5) is equal is the length of forging, l_{max} represents the maximum radius length of the forging, m is the coefficient between them. Where $x_{distance}$ in Eq. (6) is equal is the distance between each reference point, n is the number of reference points.

The reference points are random only in the y-axis

direction, and the ranges of the upper and lower parts are set to $[LB, UB]^T$, where *UB* is the 'maximum height of the forging (*maxh*) ', where *LB* is a value greater than 0. The values of *LB* and *UB* can be changed according to the requirements, thus narrowing the scope of the graphical search, and increasing efficiency. The feasible region of the design variables of the two-stage curve shall be defined as follows:

$$\begin{cases} LB^T \le [y_{11}, y_{12} \cdot\cdot y_{1n}]^T \le UB^T \\ -UB^T \le [y_{21}, y_{22} \cdot\cdot y_{2n}]^T \le -LB^T \end{cases} \quad (7)$$

Here, $y_{11}, y_{12} \cdot\cdot y_{1n}$ are the shape parameters of the upper-part-preform, $y_{21}, y_{22} \cdot\cdot y_{2n}$ are the shape parameters of the lower-part-preform.

The volume of the preform is a parameter worthy of attention in the field of forging. The increase in volume brings production costs and more volume of the flash to the increase in forming load, so it is necessary to consider the preform volume. According to the volume invariance principle of plastic forming principle, it is necessary to ensure that the volume of the preform should be the same as the volume of the forging plus the flash, so it is also necessary to impose volume constraints. Specifically, a penalty function is established for the random preform graph. When the accumulated differential volume (V_{pre}) is smaller than the volume of the forging (V_{forge}) or larger than the set threshold ($\mu * V_{forge}$), the combination of such variables or the preform shape is eliminated, and fitness $F_s = 0$.

$$V_{forge} \le V_{pre} \le \mu * V_{forge} \qquad \mu \in [1, 1.2] \quad (8)$$

As we learned from the previous section, the characteristics of NURBS determine that the graphs constructed by NURBS will not produce a sharp angle structure, so when the upper and lower curves are closed to construct the graphs, a natural rounded section will be created between the two points, which corresponds to the 'bulging' phenomenon caused by the pier diameter in the preform, see the rightmost shaded part in Fig. 3, which can be used as a flash control area. Its size could be adjusted to achieve near-net forming in the subsequent design process.

Then, in the investigation process, it is found that the generation of preform shape has strong randomness. It is easy to appear very complex shapes, and such forgings are easy to fold [42], resulting in the scrapping of forgings. As shown in Fig. 3 (a, b), the shape of the forging fluctuates violently, the height difference between the peak and valley is large, and the peak and valley regions are prone to folding. The two simulations also show that it is impossible to process or forge these preforms. The shape complexity factor is used to design preforms [43], especially for more complex mass distribution parts, which becomes more important. So, it is essential to take the shape complexity factor into account in the design of preforms. Euclidean distances have also been used to describe the complexity of preforms [42]. However, in the present study, the method is less applicable, based on which the thesis proposes a height difference shape control method. Through the analysis of three consecutive control points, a Δh is calculated, and the Δh is used as a complexity factor with the following expression (9):

$$\begin{cases} Curves_{up}: (y_{1,i+2} - y_{1,i}) - (y_{1,i+1} - y_{1,i}) > \Delta h \\ Curves_{down}: (y_{2,i+2} - y_i) - (y_{2,i+1} - y_{2,i}) < -\Delta h \end{cases} \quad (9)$$

Where, the value of Δh is related to the values of *LB, UB* and $x_{distance}$, as shown in Fig. 3(b, c, d), and the larger the value of |Δh|, the higher the probability of folding occurs (here the value of Δh is obtained from the calculation of $y_{2,1}, y_{2,2}, y_{2,3}$). The Δh is calculated by the following empirical formula, which is obtained based on a previous survey.

$$\begin{cases} \Delta h \propto [x_{distance}, UB, LB] \\ \Delta h = \dfrac{x_{distance}}{k} \qquad k = 0.5 \end{cases} \quad (10)$$

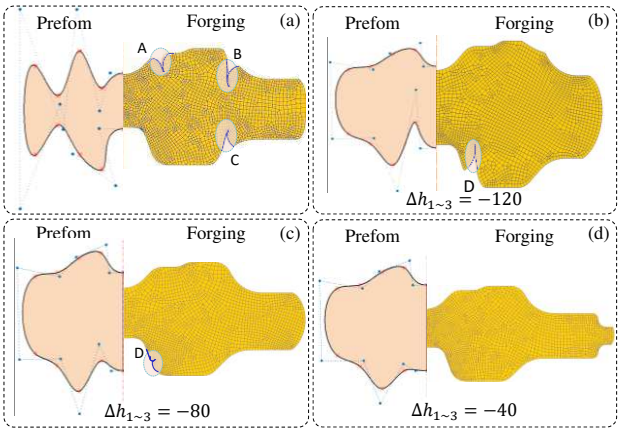

Fig. 3 Random preform design shape

In summary, the constraint model for preform shape design is established as follows:

$$\begin{cases} LB^T \le [y_{11}, y_{21} \cdot\cdot y_{1n}]^T \le UB^T \\ -UB^T \le [y_{12}, y_{22} \cdot\cdot y_{2n}]^T \le -LB^T \\ V_{forge} \le V_{pre} \le \mu * V_{forge} \quad , \quad \mu \in [1, 1.2] \\ x = m * l \qquad m \in [0.6, 0.8] \\ Curves_{up}: (y_{1,i+2} - y_{1,i}) - (y_{1,i+1} - y_{1,i}) > \Delta h \\ Curves_{down}: (y_{2,i+2} - y_i) - (y_{2,i+1} - y_{2,i}) < -\Delta h \end{cases} \quad (11)$$

2.3 FE simulation

The hot forging process was simulated by the Deform-3D commercial package. DEFORM, as a finite element simulation software, is generally operated by the user through the GUI graphical user interface of the software, as the GUI mode has the advantage of being intuitive and concise, but DEFORM software can also be run in another mode, 'Text mode', in which the user can use their edited command stream files to operate DEFORM's secondary simulation software. The text mode allows updating of graphical data in the '.key' file and submitting simulation tasks, which provides automated simulation and optimization feasibility.

3 Automatic optimization algorithms for preform

The automatic optimization algorithm takes the reference points $[y_{11}, y_{12} \cdot\cdot y_{1n}, y_{21}, y_{22} \cdot\cdot y_{2n}]^T$ as the optimization variables and the deformation uniformity as the evaluation index. The number of reference points can be set according to the complexity of the forgings. The more complex the forgings are, the more reference points can be set, but at the same time, the more complex the random preform shape will be, the longer the computation time. In addition, a virtually indefinite number of solutions are possible. Thus, choosing an appropriate optimization algorithm is necessary to solve this problem. However, finite element simulation is a typical black box, where each individual generated by the design variables has to be calculated by FEM to obtain the fitness value, which cannot be obtained by solving the mathematical model, and some optimization algorithms are no longer applicable, such as Gradient Descent, Newton's method & Newton's method, Conjugate Gradient method. GAs is possibly suitable to solve this optimization problem because genetic algorithms are population-based heuristics [44]. It is particularly suitable to deal with black-box problems that do not require auxiliary information: differentiable, derivable, and continuous. Genetic algorithm is also a stochastic optimization algorithm that excels at searching for problems with large search spaces. It can effectively use existing information to search for individuals that show promise for improving the quality of the solution. GA is similar to natural evolution. It simulates replication, crossover and, mutation in natural selection and inheritance.

An automatic, collaborative, real-time dynamic optimization process is implemented by writing the corresponding interface program using the direct communication between the finite element method and the genetic algorithm. The GA module is used as a controller to send design variables to the FEM module and receive the individual fitness returned by the FEM module. As shown in Fig. 4, the core modules in the algorithm flow chart: the preparation module, the Auto Fitness module, and the GA module. The Auto Fitness module includes several sub-modules: the preform shape modeling sub-module, the numerical simulation sub-module, and the feature extraction sub-module.

The specific process is as follows.

3.1 Module_1 Preparation

The forging forming is divided into three work steps, which are the heat transfer step, forming step and, Boolean cutting step. The heat transfer step represents the calculation of the heat transfer between the forging and the air during the removal of the preform from the furnace and its transfer to the final forging die. The forming step is the forming process of the preform in the cavity of the final forging die. The Boolean cutting step is the cutting down of the finished part from the forming forging part, which is used to observe and calculate the strain. After setting the various parameters, export the '.key' file in the first step.

Subsequently, the forging contour graph '.dxf' file is imported in MATLAB. Data is extracted to calculate the maximum height, maximum radius length, and volume of the forging to provide constraint data for the random preform shape. After selecting a suitable reference point variable matrix [*LB*, *UB*]$^{\mathrm{T}}$, the appropriate preform length coefficient m and height difference Δh are evaluated according to the variable matrix to further constrain the shape of preform and reduce its complexity.

3.2 Module_2 Auto Fitness

In this module, an automated integrated program was developed to complete the three steps of graphical modeling, numerical simulation, and feature extraction to obtain the fitness values of individuals. The operation of the whole program is based on the communication between MATLAB and Deform software. The MATLAB core commands for automated integration programs are as follows:

NURBS graphical modeling sub-module:

[NURBS, message] = GenerateGeoIGS (Y, l_{max}, V_{forge})

Numerical simulation sub-module:

```
[key, message] = system (DEF_IGS.exe <command.txt); %Generate KEY file from IGS file
[key, message] = system (DEF_PRE.exe <command.txt'); %Update KEY file
[key, message] = system (['DEF_ARM_CTL.COM', File, 'B']); % Run DB file
```

Feature target value extraction sub-module:

F = StrainUniformityArea (node, element. elementStrain,0.43,1.02); %The fitness value is calculated by equation (1)

3.3 Module_3 GA

The genetic algorithm is used to create preforms with random characteristics as an initial population, where each individual is described by a set of genes representing the control variables for the shape of the preform. Then the fitness function is calculated using the deformation uniformity parameter, and the termination condition is the preset genetic algebra. In the optimization process, the vectors of individuals with larger fitness values in the retained population are selected by changing the genes of the selected parents using crossover and variation methods, their variation variable vectors are compared with the original variable vectors and passed to the next generation, and then, the new population is evaluated again until the termination condition is satisfied. The specific algorithmic procedure can be displayed in the GA module in Fig. 4. Finally, all the optimizations have been completed, and the preforms with the above key dimensions will be determined.

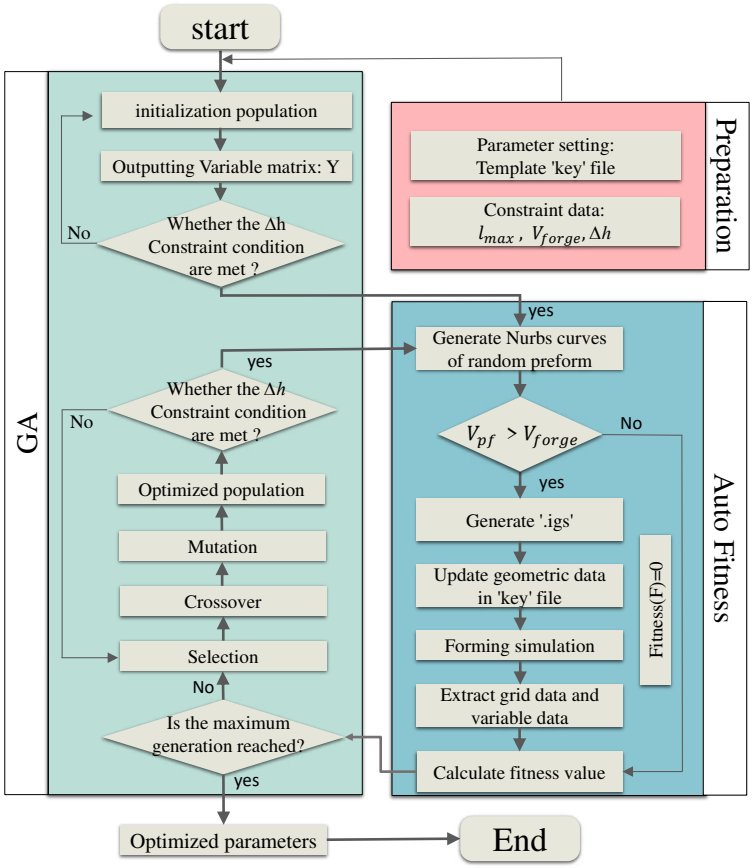

Fig 4 The automation realizes the flow chart of the integration method of the three modules, which is used to determine the optimal design parameters of the preform shape

4 Preform optimal process and results

In the following investigation, a disk forging is being used as demonstration parts, as shown in Fig. 5. Then the preform shape of this forging will be designed and optimized automatically.

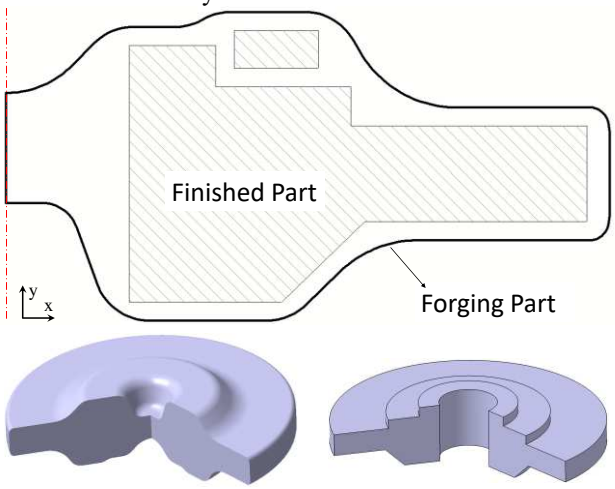

Fig. 5 Forgings drawing with forging part and finished part

4.1 Parameter definition

Finite element simulation was performed using Deform-2D. The part temperature was set to 1010°C, and the material data file IN718 [1650-2200F (900-1200C)] provided in the Deform database was used. The friction coefficient was set to 0.3, and the Heat Transfer Coefficient is 5 N/sec/mum/C. For all parameters, other parameters not explicitly stated as standard (initial parameters set by Deform) were assumed for the hot forging process.

In this research, an individual consists of 10 genes representing the design variables. It is recommended that the population size contain ten times the number of individual genes [45]. Therefore, the population size is assigned as 100, and the number of evolutionary generations is 20 as a stopping condition to reduce the total simulation time. The crossover rate is set to 0.8, and the mutation rate is set to 0.2.

Import the forging drawing shown in Fig. 5 and calculate the maximum radius length l is 323 mm, and the maximum height $maxh$ is 173 mm, the forging volume V_{forge} is 3.5225e+07 mm^3. Ten reference points are taken in the example, and the range of values of the reference point of the NURBS curve $[LB, UB]^T$ can be obtained according to $maxh$. Through preliminary exploration, constraints are defined to improve the convergence rate and avoid folding during the deformation. Since the irregularity of the parts will disappear during the optimization process, the selection range should be appropriately relaxed when setting the constraints to avoid the optimization algorithm falling into a local optimum and losing many potential combinations of variables. The specific data are shown in Table 1.

Table 1 Preform shape optimization parameters and the range of values

Constraint parameter	m	x_{pre} (6)	μ	$x_{distance}$ (8)	Δh (10)
Value	0.7	226	1.1	45.2	90

LB^T = [20, 20, 20, 20, 20, -100, -173, -173, -173, -173] ^{T}
UB^T = [100, 173, 173, 173, 173, -20, -20, -20, -20, -20] ^{T}

4.2 Results and Discussions

Figure 6 shows the development of the best-rated and average individuals within the population for 20 generations. There are 2100 simulations run for this preform optimization algorithm. Considering the time cost, the optimization was executed on an Intel Core i7 processor with four processors. Parallel Gas parallel operation was implemented by MATLAB software to improve the computing efficiency. The total time consumed from the shape design of the preform to the FEM simulation and then to the completion of the optimization was about 55 hours.

From Fig. 6, it can be found that the optimal fitness value converges quickly and surges to a higher fitness value in the 5th generation. In contrast, the average fitness is not equal to the former until after the 15th generation, which indicates that the design parameters of the preforms have a large convergence rate before the 15th generation. Then, after the 15th generation, the variation of the best fitness value and the average fitness tends to a constant value (0.9959), as shown in Table 2. This indicates that the convergence rate gradually decreases, and the search range approaches the optimal individual as the number of evolutionary generations increases. Among them, 0.9959 indicates that the area of the grid element satisfying deformation 0.43~1.02 in the finished part accounts for 99.59% of their total area, which shows that the algorithm searches for the preform shape with very good results.

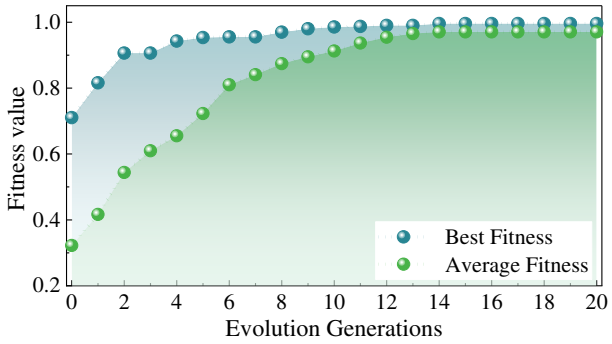

Fig. 6 Evolution curve for optimization design of preform shape using GA

The best preform shape at each generation is illustrated in Fig. 7(a-g) to easily understand the evolutionary process. With the increase of the evolutionary generation, the shape of the preform becomes more and more similar, and all of them show the shape of 'Bulging in the middle, flat on both sides'. It is not difficult to observe the data in Table 2, and the numerical changes of reference points are also getting smaller and smaller. From the equivalent strain evolution diagram in Fig. 7 (a-g), Gray, light blue, and green gradually dominate from the first generation to the fifteen generations. It shows a more uniform strain distribution in forging. Moreover, it can be seen from Fig.7 (h) that the flash rate and forming load can be reduced in the continuous evolution process, which again proves that the shape of the preform has been significantly optimized.

The histogram of the distribution of the equivalent strain (Fig. 8(a)) and the forming load-stroke diagram (Fig. 8(b)) of the finished part at the twentieth generation are presented. The distribution of the equivalent strain of the forging is nearly normal. The strain is mainly concentrated in the range of 0.65~0.85 (Fig. 8(a)), where the average value of the strain distribution (Avg) is 0.8, and the standard deviation (Stdev) is 0.1. The minimum and maximum values are 0.4 and 1.0, respectively. The maximum load during the forging process is about 30227 tons from Fig. 8(b), which meets the production requirements. The optimization results show that the genetic algorithm can automatically converge to the optimal design parameters and obtain the optimal combination of design parameters.

4.3 Redesign of optimizing the shape of preform

The optimal preform shape is obtained by the above method, and the numerical simulations are good and satisfy the optimization objectives. However, there are still some problems in practical applications, such as sharp corners caused by control points, difficult machine areas, and billet positioning structures that must be considered. Therefore, this study improves the original optimization results, based on the concept of redesign proposed in the literature [46], to find a more feasible preform shape to meet the practical application requirements while ensuring the optimization objectives.

In order to eliminate the complexity of the original optimal preform shape, the preform shape is simplified using the approximation method while maintaining the original shape characteristics, as shown in Fig. 9. Firstly, the shape of the preform was fine-tuned by changing the NURBS data points to make the preform more machinable (Fig. 9(b)). Subsequently, the number of control points was increased, and the weight values of the control points were adjusted (Fig. 9(c)) to avoid severe sharp corners, which sharp corners can cause mold penetration during simulation and stress concentration during plastic deformation. Finally, the preform shape's locating structure was designed using CAD software at the blue shaded position in Fig. 9 (d).

Table 2 Fitness value and parameter value of each generation

Item.	Fitness	The reference point of the curve above the X-axis					The reference point of the curve below the X axis				
	F	y_{11}	y_{12}	y_{13}	y_{14}	y_{14}	$-y_{21}$	$-y_{22}$	$-y_{23}$	$-y_{24}$	$-y_{25}$
1	0.816	45.6	135.3	97.3	112	31.8	47.9	143.2	135.5	93.1	108
3	0.9062	62.8	135.3	165	76.4	31.8	47.9	131.7	135.5	93.1	108
5	0.9535	60.8	135.3	165	76.4	31.8	73.7	107.2	170.4	93.1	108
9	0.9856	60.8	136.3	128.7	77.4	30.8	87.8	107.2	170.4	93.1	107
13	0.9902	59.8	136.3	128.7	77.4	30.8	-87.8	107.2	170.4	93.1	108
15	0.9959	60.8	136.3	128.7	75.6	32.8	87.8	107.2	170.4	93.1	107
20	0.9959	60.8	136.3	128.7	75.6	32.8	87.8	107.2	170.4	93.1	107

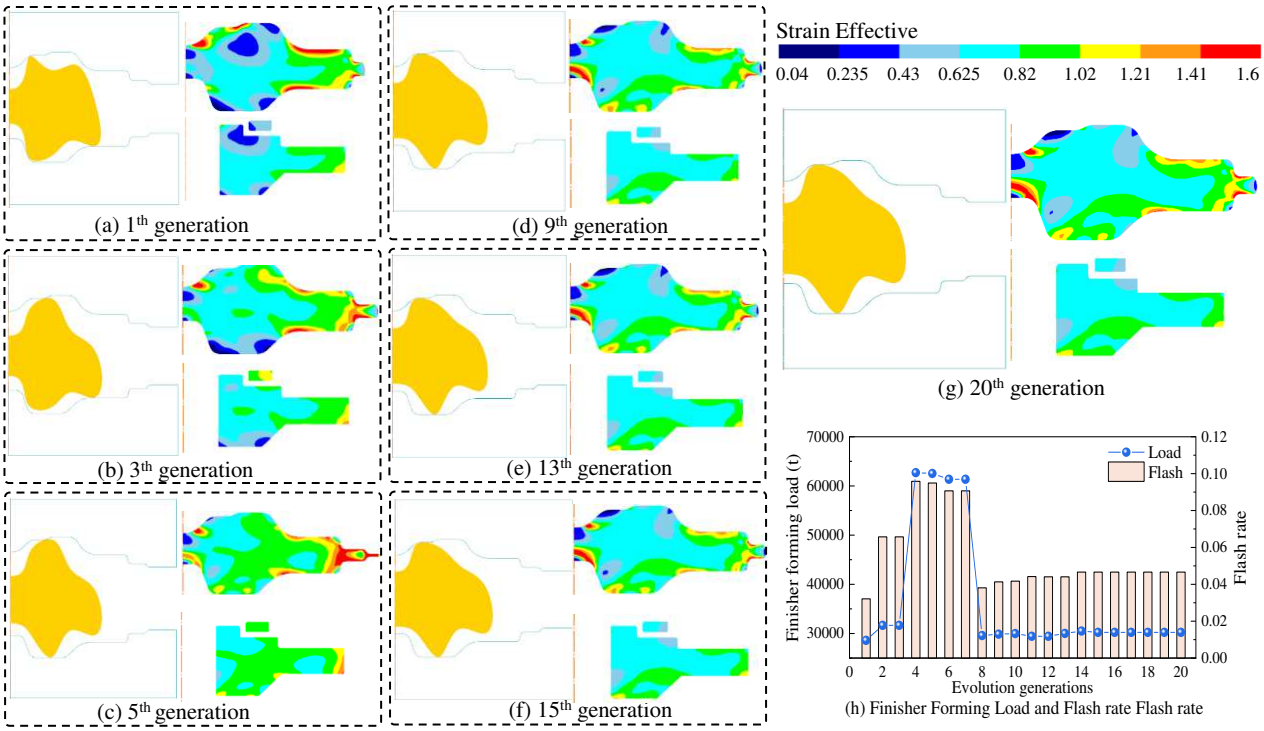

Fig. 7 The shape and equivalent strain of the best individual: (a) 1st generation, (b)3th generation, (c) 5th generation, (d) 9th generation, (e) 13th generation, (f) 15th generation
(g)20th generation, (h) Forming load and Flash rate

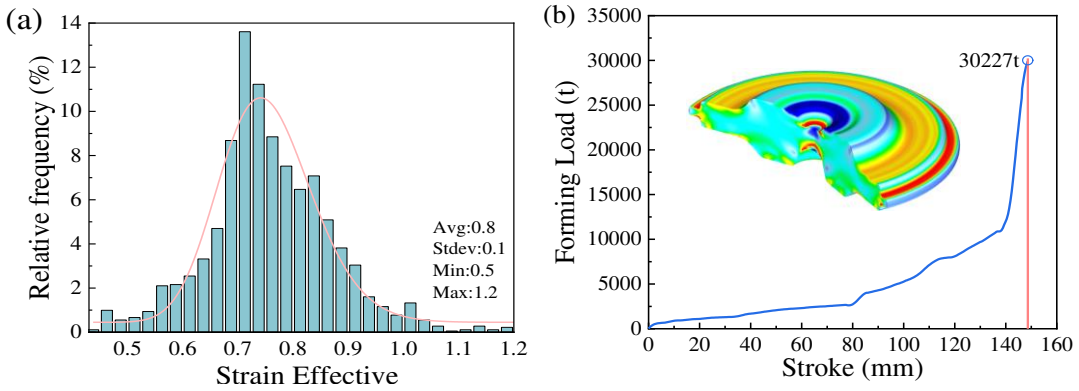

Fig. 8 The histogram of the distribution of the equivalent strain(a)and the load-stroke curve of the forming(b) at the 20th generation

The positioning of the workpiece in the die and the results are shown in Fig. 10(a-c), it can be concluded that the deformation uniformity of the redesigned preform inherits the characteristics of the original optimal one, and the equivalent strain in the 99 % area of the finished part reaches 0.43~1.02. More important is that the complexity of the preform shape is sharply lowered, making it easier to be manufactured.

In our previous work [47], the preform shape of the forging was designed by the sectional design method. 96.55% of the finished product was in the equivalent strain range of 0.43~1.02 after forging. The actual forging production was carried out for the forgings, and the forgings were able to meet the quality requirements in terms of physicochemical detection and property analysis. The grain grade in each deformation zone was above grade 10, as shown in Fig. 10(d). This shows that the preform design method and the integrated system constructed in the paper are accurate and reliable.

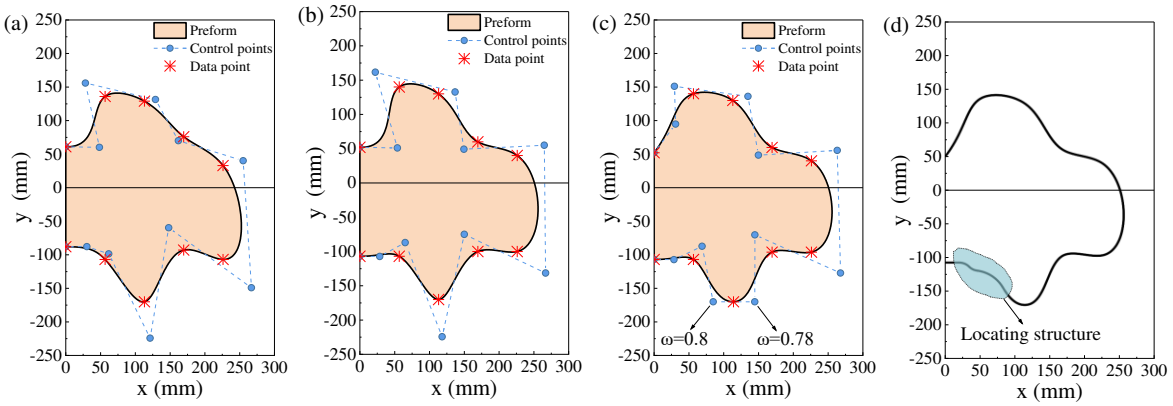

Fig. 9 Redesign of optimal preform shape: (a) Original optimal preform shape, (b) Data point modification, (c) Control point modification, (d) Locating structure

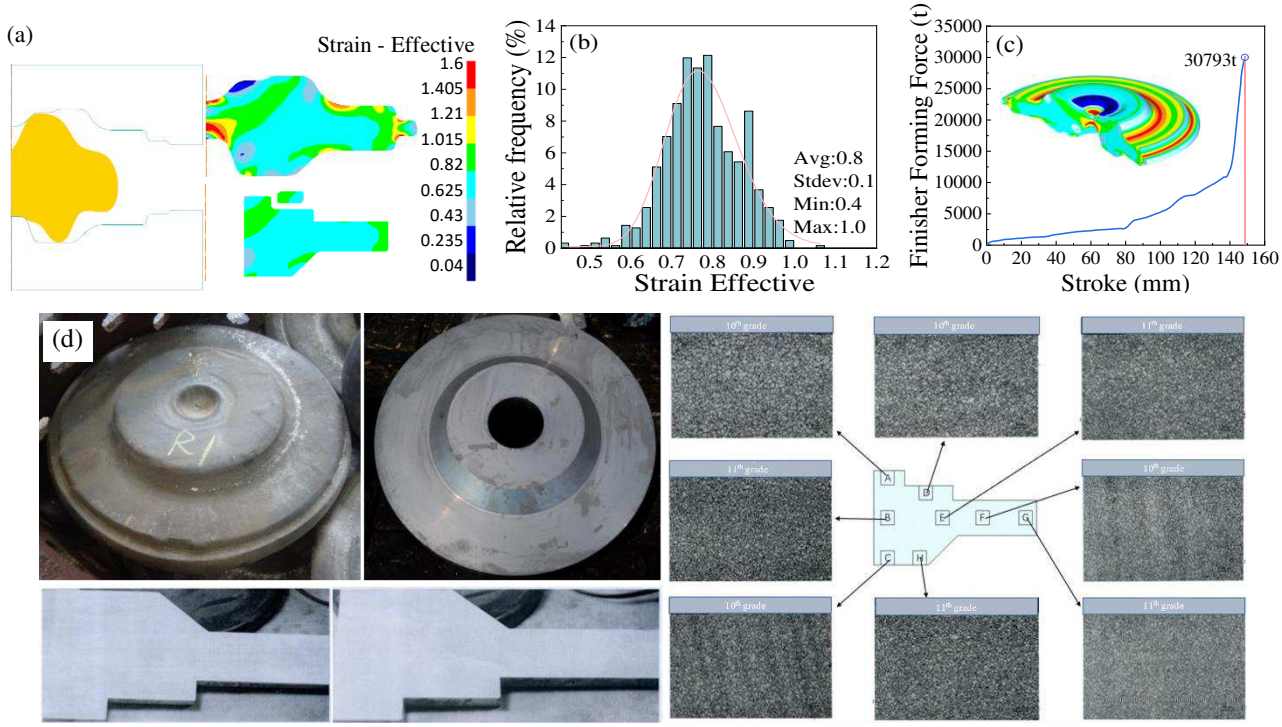

Fig. 10 Results and verification of preform redesign: (a) The shape and equivalent strain of redesigned preform, (b) Histogram of the distribution of the equivalent strain, (c) The load-stroke curve of the forming, (d) Trial production and physicochemical detection of forgings [47]

4.4 Case study

In order to better reflect the generality of the automation optimization algorithm, an aeroengine disk forging is identified as a case study in this research. The diagram of the forging is shown in Fig. 11.

The operation process is the same as the previous section and will not be repeated here. The maximum radius length l of the forging is 297mm, the maximum height $maxh$ is 94 mm, and the forging volume V_{forge} is 1.8511e+07mm^3. Other detailed data are shown in Table 3.

The forging shape contour is simple, so it takes 42 h to complete the design and optimization of the preform.

The number of finite element simulations is 2100, and the optimization results are shown in follows.

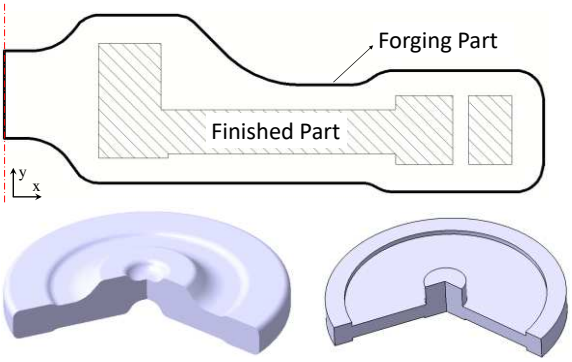

Fig. 11 A case study and its forging drawing

Table 3 Preform shape optimization parameters and the range of values

Constraint parameter	m	x_{pre} (6)	μ	$x_{distance}$ (8)	Δh (10)
Value	0.7	226	1.1	41.58	85

LB^T = [20, 20, 20, 20, 20, -94, -94, -94, -94, -94] ^{T}
UB^T = [94, 94, 94, 94, 94, -20, -20, -20, -20, -20] ^{T}

The preform shape of the aeroengine disk was obtained by the automatic optimization algorithm in the case study. After 20 generations of evolution, the fitness value of the optimal individual reached 98.30%, as shown in Table 4. From the evolution curve in Fig. 12, it is easy to see that the fitness value changes very little after the 10th generation. The optimization process can be ended at this point to improve efficiency. And the shape and equivalent strain of the best individual at each generation is illustrated in Fig. 13(a-d).

After obtaining the optimal shape of the preform, the redesign method is used to simplify the shape of the performed part, as shown in Fig. 14(a). The results show that the uniform deformation of the redesigned preform part is still well realized. The equivalent strain in the 96 % area of the finished part reaches 0.43~1.02 (Fig. 14(a,b)). Moreover, the maximum forming load is only 22082t (Fig. 14(d)), suitable for production.

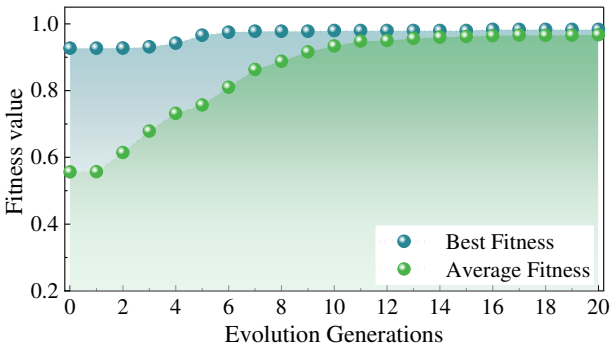

Fig. 12 Evolution curve for optimization design of preform shape using GA

Table 4 Fitness value and parameter value of each generation

Item.	Fitness	The reference point of the curve above the X-axis				The reference point of the curve below the X axis					
	F	y_{11}	y_{12}	y_{13}	y_{14}	y_{14}	$-y_{21}$	$-y_{22}$	$-y_{23}$	$-y_{24}$	$-y_{25}$
1	0.9271	84.2	54.9	46.9	51.7	43.5	71.5	66.7	54.9	57.9	82.7
5	0.9658	84.2	54.9	52.4	51.7	43.5	84.7	66.7	54.9	49.1	85.7
10	0.9797	84.4	55.9	53.4	52.7	44	83.7	67.7	54.6	50.1	85.5
15	0.9797	84.4	55.9	53.4	52.7	44	83.7	67.7	54.6	50.1	85.5
20	0.9830	84.2	55.9	53.4	52.7	43.5	83.7	67.7	54.9	50.1	85.7

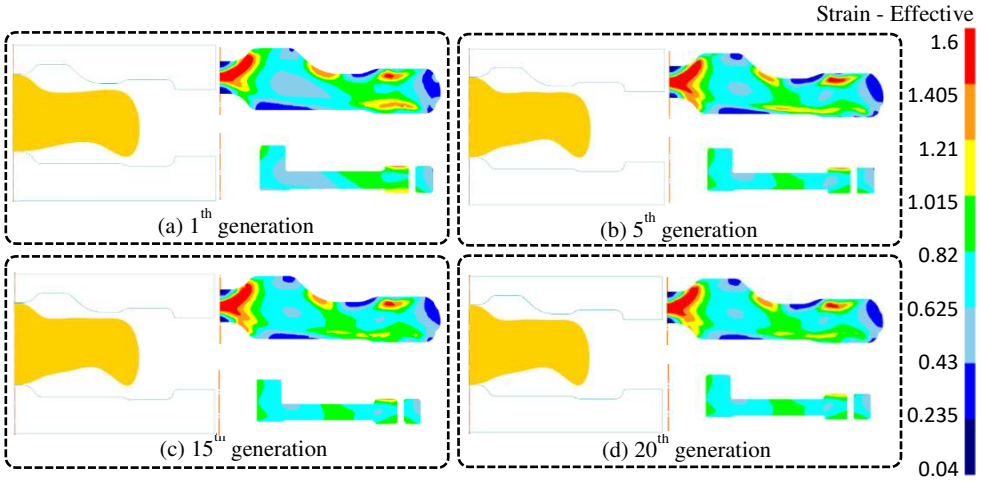

Fig. 13 The shape and equivalent strain of the best individual: (a) 1st generation, (b)5th generation, (c) 15th generation, (d) 20th generation

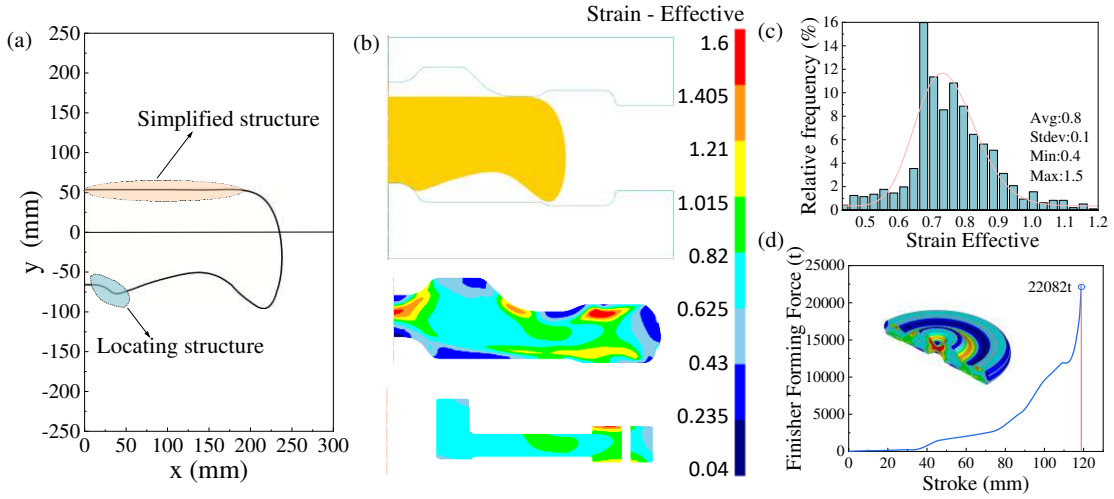

Fig. 14 Results of preform redesign at the 20th generation: (a), Redesign of optimal preform shape (b)Equivalent strain distribution, (c) Histogram of the distribution of the equivalent strain, (d) The load-stroke curve of the forming

5 Conclusion

In order to improve the quality of forgings, this paper proposes an automated preform design method based on NURBS curve modeling, finite element method analysis, and genetic algorithm optimization.

(1) The preform design method proposed can automatically complete the design and optimization of preform shape for various types of disk forgings without human intervention during the design and optimization process. The optimization process and results can be observed in real-time.

(2) The design method can optimize the preform according to specific target values. The optimization procedure can be stopped in practical use to reduce the computational cost while meeting the deformation requirements.

(3) To verify the method's effectiveness, two different engine disks are researched. The results show that the forgings have good deformation uniformity. The equivalent strain in 96.55 % and above areas of the finished parts can meet the requirements, proving the practicability and effectiveness of this method in engineering applications.

Author contribution Menghan Wang conceived and designed the experiments; Yan Han and Yifeng Chen performed the experiments; Mingfei Chen and Xiang Xiang analyzed the data; Menghan Wang and Yan Han wrote the paper.

Funding This research is supported by the Guizhou Science and Technology Cooperation Support Project [2021] General 308, and the Green Manufacturing System Integration Project of the Ministry of Industry and Information Technology (Grant No: 2018272106).

Availability of data and material Not applicable

Declarations

Competing Interests, The authors declare no competing interests.

Consent to participate All authors agreed with the consent to participate.

Consent for publication All authors have read and agreed to the published version of the manuscript.

References

1. Ding S, Wang Z, Qiu T, Zhang G, Li G, Zhou Y. (2018) Probabilistic failure risk assessment for aeroengine disks considering a transient process. Aerospace Science and Technology,78:696-707. doi: 10.1016/j.ast.2018.05.017
2. Ito E, Oka Da I, Tsukagoshi K, Muyama A, & Masa Da J. . (2010). Development of Key Technologies for the Next Generation Gas Turbine. Asme Turbo Expo: Power for Land, Sea, & Air. DOI:10.1115/GT2007-28211
3. Yanhui Y, Dong L, Ziyan H, Zijian L. (2010) Optimization of Preform Shapes by RSM and FEM to Improve Deformation Homogeneity in Aerospace Forgings. Chinese Journal of Aeronautics,23:260-267. doi: 10.1016/S1000-9361(09)60214-4
4. Tan C, Weng F, Sui S, Chew Y, Bi G. (2021) Progress and perspectives in laser additive manufacturing of key aeroengine materials. International Journal of Machine Tools and Manufacture,170:103804. doi: 10.1016/j.ijmachtools.2021.103804
5. Yanhui Y, Dong L, Ziyan H, Zijian L. (2010) Optimization of Preform Shapes by RSM and FEM to Improve Deformation Homogeneity in Aerospace Forgings. Chinese Journal of Aeronautics,23:260-267. doi: 10.1016/S1000-9361(09)60214-4
6. Sheu J, Yu C. (2009) Preform and forging process designs based on geometrical features using 2D and 3D FEM simulations. The International Journal of Advanced Manufacturing Technology,44:244-254. doi: 10.1007/s00170-008-1834-5
7. Lee S, Quagliato L, Park D, Kwon I, Sun J, Kim N. (2021) A New Approach to Preform Design in Metal Forging Processes Based on the Convolution Neural Network. Applied Sciences,11:7948. doi: 10.3390/app11177948
8. Sun W, Chen L, Zhang T, Zhang K, Zhao G, Wang G. (2018) Preform optimization and microstructure analysis on hot precision forging process of a half axle flange. The International Journal of Advanced Manufacturing Technology,95:2157-2167. doi: 10.1007/s00170-017-1377-8
9. Jin Q, Han X, Hua L, Zhuang W, Feng W. (2018) Process optimization method for cold orbital forging of component with deep and narrow groove. Journal of Manufacturing Processes,33:161-174. doi: 10.1016/j.jmapro.2018.05.007
10. Hawryluk M, Ziemba J. (2018) Application of the 3D reverse scanning method in the analysis of tool wear and forging defects. Measurement,128:204-213. doi: 10.1016/j.measurement.2018.06.037
11. Zhao J, Deng Y, Zhang J, Tang J. (2019) Effect of forging speed on the formability, microstructure and mechanical properties of isothermal precision forged of Al–Zn–Mg–Cu alloy. Materials Science and Engineering: A,767:138366. doi: 10.1016/j.msea.2019.138366
12. Gao PF, Fei MY, Yan XG, Wang SB, Li YK, Xing L, Wei K, et al. (2019) Prediction of the folding defect in die forging: A versatile approach for three typical types of folding defects. Journal of Manufacturing Processes,39:181-191. doi: 10.1016/j.jmapro.2019.02.027
13. Ko D, Kim D, Kim B. (1999) Application of artificial neural network and Taguchi method to preform design in metal forming considering workability. International journal of machine tools & manufacture,39:771-785. doi: 10.1016/S0890-6955(98)00055-8
14. Wang M, Xiao G, Li Z, Wang J. (2018) Shape optimization methodology of clinching tools based on Bezier curve. The International Journal of Advanced Manufacturing Technology,94:2267-2280. doi: 10.1007/s00170-017-0987-5
15. Li F, Chen P, Han J, Deng L, Yi J, Liu Y, Eckert J. (2020) Metal flow behavior of P/M connecting rod preform in flashless forging based on isothermal compression and numerical simulation. Journal of Materials Research and Technology,9:1200-1209. doi: 10.1016/j.jmrt.2019.11.047
16. Guan J, Wang GC, Guo T, Song LB, Zhao GQ. (2009) The microstructure optimization of H-shape forgings based on preforming die design. Materials Science and Engineering: A,499:304-308. doi: 10.1016/j.msea.2007.11.144
17. Li Y, Zhang H, Shang X, Liu M, Zhao S, Cui Z. (2022) A multiscale investigation on the preferential deformation mechanism of coarse grains in the mixed-grain structure of 316LN steel. International Journal of Plasticity,152:103244. doi: 10.1016/j.ijplas.2022.103244
18. Wang X, Huang Z, Cai B, Zhou N, Magdysyuk O, Gao Y, Srivatsa S, et al. (2019) Formation mechanism of abnormally large grains in a polycrystalline nickel-based superalloy during heat treatment processing. Acta Materialia,168:287-298. doi: 10.1016/j.actamat.2019.02.012
19. Li Y, Dlouhý J, Vavřík J, Džugan J, Konopík P, Krajňák T, Veselý J. (2022) Investigation of short-term creep properties of a coarse-grained Inconel 718 fabricated by directed energy deposition compared to traditional Inconel 718. Materials Science and Engineering: A,844:143143. doi: 10.1016/j.msea.2022.143143
20. Chang CC, Bramley AN. (2000) Forging preform design using a reverse simulation approach with the upper bound finite element procedure. ARCHIVE Proceedings of the Institution of Mechanical Engineers Part C Journal of Mechanical Engineering Science 1989-1996 (vols 203-210),214:127-136. doi: 10.1243/0954406001522868
21. Almohaileb M, Gunasekera JS. (2008) Abstract: Backward Simulations using Modified Upper Bound Elemental Technique (MUBET) for Preform Design in Forging Process. doi: http://dx.doi.org/
22. Alfozan A, Gunasekera JS. (2003) An upper bound elemental technique approach to the process design of axisymmetric forging by forward and backward simulation. Journal of Materials Processing Technology,142:619-627. doi: 10.1016/S0924-0136(03)00680-0
23. Zhao G, Wright E, Grandhi RV. (1996) Computer aided preform design in forging using the inverse die contact tracking method. International journal of machine tools & manufacture,36:755-769. doi: 10.1016/0890-6955(96)00123-X
24. Zhao G, Zhao Z, Wang T, Grandhi RV. (1998) Preform design of a generic turbine disk forging process. Journal of Materials Processing Technology,84:193-201. doi: https://doi.org/10.1016/S0924-0136(98)00221-0
25. Guan Y, Bai X, Liu M, Song L, Zhao G. (2015) Preform design in forging process of complex parts by using quasi-equipotential field and response surface methods. The International Journal of Advanced Manufacturing Technology,79:21-29. doi: 10.1007/s00170-014-6775-6
26. Tao Y, Zhou J, Cao J, Luo Y, Chen B. (2015) Optimization design preform billet shape of 7050 aluminum alloy giant plane forgings based on electric field method and MBC

toolbox. The International Journal of Advanced Manufacturing Technology,81:231-240. doi: 10.1007/s00170-015-7149-4

27. Biba N, Vlasov A, Krivenko D, Duzhev A, Stebunov S. (2020) Closed Die Forging Preform Shape Design Using Isothermal Surfaces Method. Procedia Manufacturing,47:268-273. doi: 10.1016/j.promfg.2020.04.219
28. Lee SR, Lee YK, Park CH, Yang DY. (2002) A new method of preform design in hot forging by using electric field theory. International Journal of Mechanical Sciences,44:773-792. doi: https://doi.org/10.1016/S0020-7403(02)00003-6
29. Torabi SHR, Alibabaei S, Bonab BB, Sadeghi MH, Faraji G. (2017) Design and optimization of turbine blade preform forging using RSM and NSGA II. Journal of Intelligent Manufacturing,28:1409-1419. doi: 10.1007/s10845-015-1058-0
30. WEI K, ZHAN M, FAN X, YANG H, GAO P, MENG M. (2018) Unequal-thickness billet optimization in transitional region during isothermal local loading forming of Ti-alloy rib-web component using response surface method. Chinese Journal of Aeronautics,31:845-859. doi: 10.1016/j.cja.2017.07.005
31. Meng F, Cai Z, Chen Q. (2019) Multi-objective optimization of preforming operation in near-net shape forming of complex forging. The International Journal of Advanced Manufacturing Technology,105:4359-4371. doi: 10.1007/s00170-019-04539-8
32. Shim H. (2003) Optimal preform design for the free forging of 3D shapes by the sensitivity method. Journal of Materials Processing Technology,134:99-107. doi: https://doi.org/10.1016/S0924-0136(02)00928-7
33. Shamsi-Sarband A, Hosseinipour SJ, Bakhshi-Jooybari M, Shakeri M. (2013) The Effect of Geometric Parameters of Conical Cups on the Preform Shape in Two-Stage Superplastic Forming Process. Journal of Materials Engineering and Performance,22:3601-3611. doi: 10.1007/s11665-013-0636-6
34. Kampen D, Richter J, Blohm T, Knust J, Langner J, Stonis M, Behrens B. (2020) Design of a genetic algorithm to preform optimization for hot forging processes. International Journal of Material Forming,13:77-89. doi:10.1007/s12289-019-01469-4
35. Febriani RA, Park HS, Kumar S, Lee CM. (2020) Preform Optimization of Functional Bevel Gear for Warm Forging Processes. International Journal of Automotive Technology,21:1097-1106. doi: 10.1007/s12239-020-0103-y
36. Liu C, Xu W, Wang Y, Liu M. (2021) Optimal design of preform shape based on EFA-FEM-GA integrated methodology. International Journal of Material Forming,14:1043-1056. doi: 10.1007/s12289-021-01620-0
37. Shao Y, Lu B, Ou H, Chen J. (2015) A new approach of preform design for forging of 3D blade based on evolutionary structural optimization. Structural and Multidisciplinary Optimization,51:199-211. doi: 10.1007/s00158-014-1110-2
38. Yang H, Ma X, Jiao F, Fang Z. (2019) Preform optimal design of H-shaped forging based on bi-directional evolutionary structural optimization. The International Journal of Advanced Manufacturing Technology,101:1-8. doi:10.1007/s00170-018-2906-9
39. Thiyagarajan N, Grandhi RV. (2005) Multi-level design process for 3-D preform shape optimization in metal forming. Journal of Materials Processing Technology,170:421-429. doi: 10.1016/j.jmatprotec.2005.05.051
40. Lee SR, Lee YK, Park CH, Yang DY. (2002) A new method of preform design in hot forging by using electric field theory. International Journal of Mechanical Sciences,44:773-792. doi: https://doi.org/10.1016/S0020-7403(02)00003-6
41. Piegl, Les and Tiller, & Wayne. (1997). The Nurbs Book. Springer-Verlag. doi: http://dx.doi.org/
42. Knust J, Podszus F, Stonis M, Behrens B, Overmeyer L, Ullmann G. (2017) Preform optimization for hot forging processes using genetic algorithms. The International Journal of Advanced Manufacturing Technology,89:1623-1634. doi: 10.1007/s00170-016-9209-9
43. Teterin GP, Tarnovskiy IY, Chechik AA. (1966) Shape difficulty criteria for forgings. Kuznechno-Shtampovochnoe Proizvodstvo. doi: nul
44. Katoch S, Chauhan SS, Kumar V. (2021) A review on genetic algorithm: past, present, and future. Multimedia Tools and Applications,80:8091-8126. doi: 10.1007/s11042-020-10139-6
45. Rouffaud R, Hladky-Hennion AC, Levassort F. (2017) A combined genetic algorithm and finite element method for the determination of a practical elasto-electric set for 1-3 piezocomposite phases. Ultrasonics,77:214-223. doi: 10.1016/j.ultras.2017.02.015
46. Tang Y, Zhou X, Chen J. (2008) Preform tool shape optimization and redesign based on neural network response surface methodology. Finite Elements in Analysis and Design,44:462-471. doi: 10.1016/j.finel.2008.01.007
47. Wang M, Xiang X, Li S, Hu Y. (2021) Pre-forming design method and its automation realization based on forming law of aviation disc. Journal of Central South University（Science and Technology),52:3429-3438. doi: 10.11817/j.issn.1672-7207.2021.10.006